



***ELECTROCHEMICAL ANALYSIS OF CARBON NANOTUBES/TITANIUM
DIOXIDE COMPOSITE MODIFIED GLASSY CARBON ELECTRODE***

GANCHIMEG PERENLEI

FS 2010 40

**ELECTROCHEMICAL ANALYSIS OF CARBON NANOTUBES/TITANIUM
DIOXIDE COMPOSITE MODIFIED GLASSY CARBON ELECTRODE**



By

GANCHIMEG PERENLEI

**Thesis Submitted to the School of Graduate Studies, Universiti Putra Malaysia in
Fulfilment of the Requirements for the Degree of Master of Science**

OCTOBER 2010

Abstract of this thesis presented to the Senate of Universiti Putra Malaysia in fulfilment of the requirements for the degree of Master of Science

ELECTROCHEMICAL ANALYSIS OF CARBON NANOTUBES/TITANIUM DIOXIDE COMPOSITE MODIFIED GLASSY CARBON ELECTRODE

By

GANCHIMEG PERENLEI

October 2010

Chair : Associate Professor Tan Wee Tee, PhD

Faculty : Science

The new chemically modified electrode based on carbon nanotubes/titanium dioxide (CNT/TiO₂) composite modified glassy carbon electrode (GCE) was fabricated by two different (i) mechanical attachment and (ii) solvent casting methods. The CNT/TiO₂/GCE composite has been characterized using voltammetric techniques of linear sweep voltammetry, cyclic voltammetry, chronoamperometry and chronocoulometry in this work. The surface morphology of the CNT/TiO₂ composite film was studied by scanning electron microscopy and the percentage of the elements in components was examined by energy dispersive X-ray.

The CNT/TiO₂/CGE was applied in the electrochemical determination of 0.5 mM ascorbic acid in 0.1 M NaCl (pH 6.2), 0.1 mM potassium ferricyanide in 0.1 M Na₂HPO₄ (pH 8.5) and 0.2 mM paracetamol in 0.1 M PBS (pH 7.0). The current enhancements of 5.0 folds for the oxidation of ascorbic acid, 3.0-3.1 folds for the redox of potassium ferricyanide and 8.5-11.0 folds for the redox of paracetamol were obtained using the CNT/TiO₂/GCE when compared with unmodified GCE. The responses of each analyte at various electrodes are in the order:

$$\text{CNT/TiO}_2/\text{GCE} > \text{CNT/GCE} > \text{GCE} > \text{TiO}_2/\text{GCE}$$

Under the optimized parameters, the linear calibration graph showed correlation coefficient of 0.997 for the oxidation of 0.05-2 mM ascorbic acid, 0.999 for the redox of 0.01-0.2 mM potassium ferricyanide and the concentration isotherm of paracetamol in the range of 0.01 - 2 mM, with linearity of up to 1.2 mM. From this calibration plot, high sensitivity response of 45 $\mu\text{A}/\text{mM}$ with detection limit of 7.8 μM (100 mV/s scan rate) for the oxidation of ascorbic acid; 68.9-77.6 $\mu\text{A}/\text{mM}$ with 1.1 μM (5 mV/s) for the redox of potassium ferricyanide; and 89.94-111.3 $\mu\text{A}/\text{mM}$ with 3.9 μM (5 mV/s) for the redox of paracetamol at the CNT/TiO₂/GCE were obtained. Effect of scan rate of ascorbic acid was studied in the ranges of 10-300 mV/s, and linear relation was observed up to 70 mV/s. Based on the log plot of oxidation current vs. scan rate, an experimental slope of 0.45 was obtained, which is very close to the theoretical value of 0.5, indicating that the current is under diffusion controlled. Based on redox currents of potassium ferricyanide vs. potential plot, the zero-current potentials were obtained at $E_{pa}^o=209$ mV and $E_{pc}^o=189$ mV in the scan rates ranges of 10-600 mV/s. Diffusion

coefficient was calculated as $1.52 \times 10^{-5} \text{ cm}^2/\text{s}$ from the chronocoulometry study and an activation energy obtained was 6 kJ/mol in the presence of potassium ferricyanide in aqueous media at the composite electrode. The redox peak currents of paracetamol were significantly dependent on dosages of CNT to TiO_2 in the composite at GCE. The recovery experiment of paracetamol in commercially available samples was carried out and the recovery rates of $95 \pm 2\%$ and $96 \pm 2\%$ were found using the CNT/ TiO_2 /GCE. The results revealed that the electrochemical ability of CNT is improved when combined with TiO_2 nanoparticles as a composite. The use of the CNT/ TiO_2 /GCE is highly sensitive, selective and stable in electrochemical measurement.

Abstrak tesis yang dikemukakan kepada Senat Universiti Putra Malaysia sebagai memenuhi keperluan untuk ijazah Master Sains

**ANALISIS ELEKTROKIMIA KOMPOSIT KARBON KACA TERUBAHSUAI
KARBON NANOTIUB/TITANIUM DIOKSIDA**

Oleh

GANCHIMEG PERENLEI

Oktober 2010

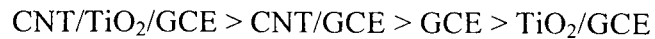
Pengerusi : Profesor Madya Tan Wee Tee, PhD

Fakulti : Sains

Electrod kimia terubahsuai berdasarkan nanotube karbon/titanium dioksida (CNT/TiO₂) komposit elektrod karbon yang diubahsuai kaca (GCE) telah dibuat dgn 2 kaedah berbeza (i) lekatan mekanikal (ii) kaedah tuangan pelarut. Komposit CNT/TiO₂/GCE telah dianalisis menggunakan teknik voltametri dari linear sweep voltametri kadar linear, voltametri siklik, chronoamperometri dan chronocoulometri. Morfologi permukaan filem komposit CNT/TiO₂ dianalisa dengan imbasan mikroskop elektron dan peratusan elemen dalam komponen dianalisa oleh tenaga sinar-X dispersif.

CNT/TiO₂/GCE digunakan dalam penentuan elektrokimia 0.5 mM asid askorbik dalam 0.1 M NaCl (pH 6.2), 0.1 mM kalium ferricyanide dalam 0.1 M Na₂HPO₄ (pH 8.5) dan parasetamol 0.2 mM dalam 0.1 M PBS (pH 7.0). Pertambahan arus sebanyak 5.0 kali

ganda untuk pengoksidaan asid askorbik, 3.0-3.1 kali ganda untuk redoks kalium ferrisianida dan 8.5-11.0 kali ganda untuk redoks parasetamol diperolehi dengan menggunakan CNT/TiO₂/GCE apabila dibandingkan dengan GCE tanpa ubah suai. Respon analit masing-masing pada pelbagai elektrod adalah dalam urutan:



Berdasarkan parameter yang dioptimumkan, graf kalibrasi linear menunjukkan pekali korelasi 0.997 untuk pengoksidaan 0.05-2 mM asid askorbik, 0.999 untuk redoks 0.01-0.2 mM kalium ferrisianida dan isoterm konsentrasi parasetamol dalam julat 0.01 - 2 mM, dengan julat linear hingga 1.2 mM. Dari plot kalibrasi, sensitiviti response adalah tinggi sebanyak 45 $\mu\text{A}/\text{mM}$ dengan limit pengesanan 7.8 μM (100 mV/s kadar imbasan) untuk pengoksidaan asid askorbik; 68.9-77.6 $\mu\text{A}/\text{mM}$ dengan 1.1 μM (5 mV/s) untuk redoks kalium ferrisianida; dan 89.94-111.3 $\mu\text{A}/\text{mM}$ dengan 3.9 μM (5 mV/s) untuk redoks parasetamol di CNT/TiO₂/GCE diperolehi. Pengaruh kadar imbasan asid askorbik dipelajari dalam julat 10-300 mV/s, dan hubungan linear diperolehi sehingga 70 mV/s. Berdasarkan plot log arus pengoksidaan vs. kadar imbasan, kecerunan eksperimen 0.45 diperolehi, yang menghampin nilai teori iaitu 0.5, menunjukkan bahawa arus ini di bawah difusi terwakal. Berdasarkan arus redoks plot kalium ferrisianida melawan potensi, arus potensi sifar diperolehi pada $E_{pa}^o=209$ mV dan $E_{pc}^o=189$ mV dengan kadar imbasan 10-600 mV/s. Pekali difusi dikira sebagai 1.52×10^{-5} cm²/s daripada kajian chronocoulometri dan tenaga pengaktifan yang diperolehi adalah 6 kJ/mol dengan kehadiran kalium ferrisianida dalam media akues pada elektrod komposit. Arus puncak redoks parasetamol secara signifikannya bergantung pada dos

CNT pada TiO_2 dalam komposit pada CGE. Kajian aplikasi untuk parasetamol dalam sampel yang tersedia secara komersil dilakukan dan tahap pemulihan dari $95\pm 2\%$ dan $96\pm 2\%$ dijumpai menggunakan CNT/ TiO_2 /GCE tersebut. Keputusan kajian menunjukkan bahawa kemampuan elektrokimia CNT dipertingkatkan bila digabungkan dengan nanopartikel TiO_2 sebagai komposit. CNT/ TiO_2 /GCE ini sangat sensitif, selektif dan stabil dalam pengukuran electrokimia.



ACKNOWLEDGEMENTS

I would like to give my deepest thanks to God Almighty from my heart. My deep respect and appreciation is expressed to my supervisor Assoc. Prof. Dr. Tan Wee Tee for his enthusiastic supervision, continuous guidance, kind encouragement and friendly advices throughout my study. I wish to convey my sincere thanks to my supervisory committee members Assoc. Prof. Dr. Nor Azah Yusof and Dr. Goh Joo Kheng for their valuable suggestions, constructive comments, and support.

I wish to offer my special thanks to my beloved family: father-Perenlei, mother-Oyun-Ukhaan, grandmother-Yumsenge, aunt-Oyunchimeg, all brothers and relatives for their love, understanding, constant financial and moral support, and inspiration to complete my Masters' degree successfully.

I am also grateful to my colleagues, especially Farhan, Mira, Yaw, Erina, Huda, Radhi and Zidan for their guidance and help during this time. My acknowledgement goes to UPM and MOSTI for providing the research fund and facilities.

My sincere thanks is extended to all my friends, especially Amin, Fadumo, Wendy, Tesfa, Veno, Yusuf, Adamu, Ibrahim and Roshidul for their kindness, encouragement, friendship and help. I am also very thankful for all members of PSG, PGF, UPMISA and Christian churches to have a great time in Malaysia.

TABLE OF CONTENTS

	Page
ABSTRACT	ii
ABSTRAK	v
ACKNOWLEDGEMENTS	viii
APPROVAL	ix
DECLARATION	xi
LIST OF TABLES	xv
LIST OF FIGURES	xvi
LIST OF SYMBOLS	xx
LIST OF ABBREVIATIONS	xxii
CHAPTER	
1 INTRODUCTION	1
1.1 Chemically Modified Electrode	1
1.2 Nanostructured Material Modified Electrode	2
1.3 Carbon Nanotubes	3
1.4 Titanium Dioxide	4
1.5 Ascorbic Acid	5
1.6 Paracetamol	6
1.7 Fundamental of Voltammetric Techniques	7
1.7.1 Linear Sweep Voltammetry	8
1.7.2 Cyclic Voltammetry	9
1.7.3 Chronoamperometry	11
1.7.4 Chronocoulometry	12
1.8 Problem Statement	15
1.9 Objectives	16
2 LITERATURE REVIEW	17
2.1 Carbon Nanotubes	17
2.2 Titanium Dioxide	19
2.3 Carbon Nanotubes/Titanium Dioxide Composite	22
3 EXPERIMENTAL	29
3.1 Materials and Reagents	29
3.2 Instrumentation and Apparatus	30

3.3	General Procedure	32
3.4	Preparation of Modified Electrode	33
3.5	Experimental Parameter's Procedure	34
3.5.1	Effect of Enhancement Study	34
3.5.2	Effect of Potential Cycling	35
3.5.3	Effect of Varying pH	35
3.5.4	Effect of Varying Dosage	36
3.5.5	Effect of Varying Supporting Electrolyte and Its Concentration	36
3.5.6	Effect of Varying Scan Rate	37
3.5.7	Effect of Varying Temperature	37
3.5.8	Effect of Varying Concentration of Analyte	38
3.5.9	Chronoamperometry and Chronocoulometry	39
3.5.10	Recovery Study	39
3.5.11	Scanning Electron Microscopy	40
3.5.12	Energy Dispersive X-ray	40
4	RESULTS AND DISCUSSION	41
4.1	Determination of Ascorbic Acid at the CNT/TiO ₂ /GCE via MAM	41
4.1.1	Current Enhancement Study	42
4.1.2	Effect of Potential Cycling	44
4.1.3	Effect of pH	45
4.1.4	Effect of Varying Scan Rate	46
4.1.5	Effect of Varying Supporting Electrolytes	48
4.1.6	Calibration Graphs	49
4.1.7	Effect of Varying Temperature	51
4.1.8	Chronoamperometry and Chronocoulometry Study	53
4.1.9	Recovery Study	55
4.2	Determination of Ascorbic Acid at the CNT/TiO ₂ /GCE via SCM	56
4.2.1	Current Enhancement Study	56
4.2.2	Effect of Scan Rate	58
4.2.3	Effect of pH	59
4.2.4	Calibration Graph	60
4.2.5	Effect of Supporting Electrolyte Concentration	61
4.3	Electrochemical Detection of Potassium Ferricyanide at the CNT/TiO ₂ /GCE	62
4.3.1	Peak Current Enhancement	62
4.3.2	Number of Scanning	64
4.3.3	Effect of Varying pH	65
4.3.4	Effect of Varying Scan Rate	67

4.3.5	Effect of Varying Concentration of Potassium Ferricyanide	69
4.3.6	Effect of Varying Temperature	71
4.3.7	Chronoamperometry Study	73
4.3.8	Chronocoulometry Study	74
4.4	Electrochemical Detection of Paracetamol at the CNT/TiO ₂ /GCE	75
4.4.1	Peak Current Enhancement of Paracetamol	75
4.4.2	Effect of Varying pH	77
4.4.3	Effect of Varying Dosages of Components	80
4.4.4	Effect of Varying Scan Rate	82
4.4.5	Calibration Graph	85
4.4.6	Paracetamol Determination /Recovery Study	88
4.5	Scanning Electron Microscopy Study	89
4.6	Energy Dispersive X-Ray Study	90
5	CONCLUSIONS	91
	RECOMMENDATIONS FOR FUTURE RESEARCH	92
	REFERENCES	93
	APPENDICES	98
	BIODATA OF STUDENT	103

LIST OF TABLES

Table	Page
4.1 Recovery rates of ascorbic acid (0.05 mM and 1 mM) spiked into rose syrup sample in 0.1 M KCl using the CNT/TiO ₂ /GCE	55
4.2 Obtained peak currents of 0.2 mM paracetamol on the different dosages (volume) of components (CNT/DMF and TiO ₂ /Water) in the composite of the CNT/TiO ₂ /GCE	81
4.3 Recovery rates of paracetamol (0.2 mM) extracted from commercially paracetamol tablet samples in 0.1 M PBS using the CNT/TiO ₂ /GCE	88
4.4 Percentage of various elements before and after electrolysis	90
5.1 The obtained oxidation peak potentials and currents at the various electrodes in the presence of 0.5 mM ascorbic acid in 0.1 M KCl	98
5.2 The obtained peak potentials and currents for the oxidation of 0.5 mM ascorbic acid on the different pH conditions using the CNT/TiO ₂ composite modified GCE via MAM	98
5.3 The oxidation peak potentials and currents of 0.5 mM ascorbic acid in 0.1 M KCl were obtained at CNT/TiO ₂ /GCE via MAM with different scan rates	99
5.4 The varying temperature towards peak current and potential was obtained at the CNT/TiO ₂ /GCE via MAM for the oxidation of 0.5 mM ascorbic acid	99
5.5 The obtained redox peak potentials and currents at the various electrodes in the presence of 0.1 mM potassium ferricyanide in 0.1 M Na ₂ HPO ₄ solution	100
5.6 The redox peak currents and potentials were recorded on the varying concentrations of potassium ferricyanide using the CNT/TiO ₂ /GCE	100
5.7 The obtained peak currents and potentials for the redox process of 0.2 mM paracetamol in aqueous media at various electrodes	101
5.8 Table of scan rates, peak currents and potentials of 0.2 mM paracetamol in 0.1 M PBS at the CNT/TiO ₂ /GCE	101
5.9 The experimental values of peak potential and current for the different concentration of paracetamol in PBS using the CNT/TiO ₂ modified GCE	102

LIST OF FIGURES

Figure		Page
1.1	Scheme of single-walled (a) and multi-walled (b) carbon nanotubes	3
1.2	TiO ₂ crystal structures: tetragonal (a), tetragonal (b) and orthorhombic (c)	4
1.3	Molecular structure of ascorbic acid	5
1.4	Molecular structure of paracetamol	6
1.5	Linear sweep voltammetry	8
1.6	Triangular potential waveform for cyclic voltammetry	9
1.7	Potential waveform for chronoamperometry	11
1.8	Chronocoulogram (charge-time) response for double potential step chronocoulometry	13
3.1	Schematic diagram of the instrumental arrangement	30
3.2	Set up for voltammetric cell system	31
3.3	Preparation of the CNT/TiO ₂ composite modified GCE	34
4.1	Overlapping graph of voltammograms obtained for the oxidation of 0.5 mM ascorbic acid in 0.1 M KCl at the various electrodes of: CNT/TiO ₂ /GCE (a); CNT/GCE (b); GCE (c) and TiO ₂ /GCE (d) after background subtracted and with a scan rate of 100 mV/s	42
4.2	CV of potential cycling for the oxidation of 0.5 mM ascorbic acid at the CNT/TiO ₂ /GCE in 0.1 M KCl with a scan rate of 100 mV/s for 10 cycles	44
4.3	A plot of the dependence of pH value for the oxidative current of 0.5 mM ascorbic acid in 0.1 M KCl mediated by the CNT/TiO ₂ /GCE at different pHs of 2.0 – 9.0	45
4.4	CV obtained for the oxidation of ascorbic acid in 0.1 M KCl at the CNT/TiO ₂ /GCE with different scan rates of 10 mV/s to 1000 mV/s	46

4.5	A plot of log scan rate against log oxidation peak current of ascorbic acid using the CNT/TiO ₂ /GCE immersed in 0.1 M KCl electrolyte at 25°C and with scan rates ranging from 10 mV/s to 1000 mV/s	47
4.6	Overall graph (background subtracted) of the oxidation current of ascorbic acid at the CNT/TiO ₂ /GCE in different supporting electrolytes at 25°C with a scan rate of 100 mV/s	48
4.7	CVs obtained at the CNT/TiO ₂ mechanically attached on CGE with different concentration of ascorbic acid (0.05 mM to 2.5 mM) in 0.1 M KCl with a scan rate of 100 mV/s	49
4.8	A plot showing the dependence of the oxidation current on different concentration of ascorbic acid in 0.1 M KCl solution at the CNT/TiO ₂ /GCE	50
4.9	CVs obtained for the 0.5 mM ascorbic acid at the CNT/TiO ₂ /GCE at various temperatures of 10°C - 80°C and with a scan rate of 100 mV/s	51
4.10	A plot of ln I _{pa} against 1/T K ⁻¹ for the CNT/TiO ₂ /GCE in the presence of 0.5 mM ascorbic acid in 0.1 M KCl	52
4.11	Chronoamperogram of ascorbic acid at the CNT/TiO ₂ /GCE in 0.1 M KCl solution at 25°C with 250 ms pulse width	53
4.12	A chronocoulogram shows the rising current time transient with maximum at the oxidation wave	54
4.13	Voltammograms obtained for the oxidation of 0.5 mM ascorbic acid in 0.1 M NaCl using the CNT/TiO ₂ /GCE (a); CNT/GCE (b); TiO ₂ /GCE (c); GCE (d) and GCE (e) with a scan rate of 100 mV/s	57
4.14	A plot of log scan rate against log peak current for the oxidation of 0.5 mM ascorbic acid on the surface of the CNT/TiO ₂ /GCE with different scan rates of 10 mV/s - 70 mV/s	58
4.15	A plot of pH against oxidation peak current of 0.5 mM ascorbic acid at the CNT/TiO ₂ /GCE with different pH conditions of pH 2.0 – pH 8.0	59
4.16	The dependence of the oxidation current of ascorbic acid on different concentration ranging from 0.05 mM to 5 mM at the CNT/TiO ₂ /GCE	60
4.17	CV of the 0.5 mM of ascorbic acid in NaCl supporting electrolyte with various concentration ranges of 0.1 M - 4 M at the CNT/TiO ₂ /GCE	61

4.18	CVs were obtained for the 0.1 mM potassium ferricyanide in 0.1 M Na ₂ HPO ₄ at the CNT/TiO ₂ /GCE (a); CNT/GCE (b); TiO ₂ /GCE (d) and GCE (c) with a scan rate of 100 mV/s	63
4.19	CV of 10 potential cycling for the redox process of 0.1 mM potassium ferricyanide in 0.1 M Na ₂ HPO ₄ at the CNT/TiO ₂ /GCE; scan rate of 100 mV/s	64
4.20	A plot of the pH against the redox peak current of 0.1 mM potassium ferricyanide at the CNT/TiO ₂ /GCE with various pH solutions (5.0 -12.0)	65
4.21	A plot of the pH against redox peak potential of potassium ferricyanide in 0.1 M Na ₂ HPO ₄ at the CNT/TiO ₂ /GCE	66
4.22	CVs of 0.1 mM potassium ferricyanide in 0.1 M Na ₂ HPO ₄ at the CNT/TiO ₂ /GCE with different scan rates of 10 mV/s - 600 mV/s	67
4.23	A plot of the log peak current of potassium ferricyanide against log of scan rate (10 mV/s - 600mV/s) at the CNT/TiO ₂ /GCE	68
4.24	A plot of the peak of potassium ferricyanide current against peak potential with different scan rates of 10 mV/s - 600mV/s at the CNT/TiO ₂ /GCE	68
4.25	CV of potassium ferricyanide with different concentration of 0.01 mM - 0.2 mM at the CNT/TiO ₂ /GCE in 0.1 M Na ₂ HPO ₄ with a scan rate of 100 mV/s	69
4.26	The dependence of peak current against concentration of potassium ferricyanide ranges of 0.01 mM - 0.2 mM	70
4.27	CVs obtained for the redox of potassium ferricyanide using the CNT/TiO ₂ /GCE in 0.1 M Na ₂ HPO ₄ at various temperatures of 10- 80°C	71
4.28	A plot of ln peak current against 1/T K ⁻¹ for the CNT/TiO ₂ /GCE in the presence of 0.1 mM potassium ferricyanide in aqueous media	72
4.29	Chronoamperogram of 0.1 mM potassium ferricyanide in 0.1 M Na ₂ HPO ₄ using the CNT/TiO ₂ /GCE at 25°C with 250 ms pulse width	73
4.30	Chronocoulogram of 0.1 mM potassium ferricyanide in 0.1 M Na ₂ HPO ₄ at the CNT/TiO ₂ /GCE at 25°C with 250 ms pulse width	74
4.31	CVs of 0.2 mM paracetamol in 0.1 M PBS (pH 7.0) at the CNT/TiO ₂ /GCE (a); CNT/GCE (b); GCE in the presence of analyte (c) and GCE in the absence of analyte (d)	76

4.32	A plot of the redox peak currents of 0.2 mM paracetamol on different pH solutions of pH 2.0- pH 12.0	78
4.33	CVs of 0.2 mM paracetamol at the CNT/TiO ₂ /GCE film using pH buffer solutions of pH 6.0 (a); pH 7.0 (b); pH 8.0 (c); 10.0 (d) with a scan rate of 100 mV/s	78
4.34	The dependence of the peak potentials on the different pH of electrolyte solutions ranging from pH 2.0 to pH 12.0	79
4.35	CVs of 0.2 mM paracetamol redox currents at different dosages of components in the CNT/TiO ₂ /GCE composite: 30 μL CNT/5 μL TiO ₂ (a); 25μL CNT/5μL TiO ₂ (b); 20μL CNT/5μL TiO ₂ (c); 15μL CNT/5μL TiO ₂ (d); 10μL CNT/5μL TiO ₂ (e); 5μL CNT/5μL TiO ₂ (j) and 5μL CNT/10μL TiO ₂ (g)	80
4.36	CVs of 0.2 mM paracetamol at the CNT/TiO ₂ /GCE composite film in PBS (pH 7) using different scan rates of 5 mV/s to 600 mV/s	82
4.37	The dependence of the oxidation peak current of paracetamol on the log scan rates at the CNT/TiO ₂ /GCE with different scan rates of 5 mV/s - 600 mV/s	83
4.38	A plot of the redox peak current against peak potential of paracetamol at the CNT/TiO ₂ /GCE with different scan rates of 5 mV/s - 600 mV/s	84
4.39	CVs of paracetamol at the CNT/TiO ₂ /GCE composite film with different concentrations ranging from 0.01 mM to 2 mM in PBS (pH 7.0) with a scan rate of 100 mV/s	86
4.40	Calibration curve for the determination of paracetamol with various concentration ranging from 0.01 mM to 2 mM at the CNT/TiO ₂ /GCE	86
4.41	A plot of the redox peak currents on the different concentrations of paracetamol ranges of 0.01 mM - 1.2 mM at the CNT/TiO ₂ /GCE	87
4.42	A plot of peak potential on the concentration (0.01 mM – 2 mM) of paracetamol at the CNT/TiO ₂ /GCE	87
4.43	SEM images of of the CNT/TiO ₂ composite surface at the BPPGE before (a, c) and after electrolysis (b, d) at magnifications of 500 and 10,000 times	89
4.44	EDX spectrograms of elements in the CNT/TiO ₂ composite mechanically attached to a BPPGE before (a) and after electrolysis (b)	90

LIST OF SYMBOLS

A	Electrode surface area (cm^2)
C	Concentration of the analyte in the bulk solution (mole/cm^3)
D	Diffusion coefficient (cm^2/s)
D^0	Initial diffusivity of the material
e^-	Electron transferred or involved in the reaction
E	(a) Potential of an electrode (V) (b) Peak potential (V)
$E_{1/2}$	Measure half-wave potential in voltammetry (V)
E_a	Activation energy (kJ/mol)
E_i	Initial potential (V)
E_f	Final potential (V)
E_p	Peak potential (V)
E_{pa}	Anodic peak potential (V)
E_{pc}	Cathodic peak potential (V)
E^0	(a) Standard potential of an electrode (b) Standard emf for a half cell reaction
ΔE^0	Difference in standard potentials for two couples ($E_1^0 - E_2^0$) (V)
ΔE_p	Separation between the peak potentials $ E_{pa} - E_{pc} $ (V)
F	Faraday constant, charge on one mole of electrons
I_f	Faradaic current (A)
I_p	Peak current (A)

I_{pa}	Anodic peak current (A)
I_{pa}/I_{pc}	Anodic-to-cathodic peak current ratio
I_{pc}	Cathodic peak current (A)
K	(a) Constant; (b) Equilibrium constant
m	Slope
n	(a) Number of electron transfer (equiv/mole) (b) Number of electrons exchanged between one ion or molecule of a reactant and the electrode (equiv/mole)
n_a	Number of electrons involved in the rate determining step (equiv/mole)
Q	Charge (Coulomb)
Q_d	Capacitive charge (double layer), (Coulomb)
R	Gas constant
R^2	Correlation coefficient
t	Time (s)
T^0	Absolute temperature ($^{\circ}\text{C}$)
v	Scan rate (V/s)
τ	Forward step width (s)
Γ	Surface excess of reactant (mole/cm^2)
σ	Conductivity
σ^0	Standard conductivity of the material
δ	Standard deviation

LIST OF ABBREVIATIONS

Ag/AgCl	Silver-silver chloride reference electrode
BAS	Bioanalytical Systems
BPPGE	Basal plane pyrolytic graphite electrode
CA	Chronoamperometry
CC	Chronocoulometry
CE	Counter electrode
CME	Chemically modified electrode
CNT	Carbon nanotubes
CNT/TiO ₂	Carbon nanotubes/titanium dioxide
CNT/TiO ₂ /GCE	Carbon nanotubes/titanium dioxide/glassy carbon electrode
CV	Cyclic voltammogram
CVD	Chemical vapor decomposition
DMF	Dimethylformamide
EDX	Energy dispersive of X-ray
GCE	Glassy carbon electrode
KCl	Potassium chloride
KClO ₄	Potassium perchlorate
KH ₂ PO ₄	Potassium dihydrogen orthophosphate
K ₂ SO ₄	Potassium sulphate
LSV	Linear sweep voltammogram

MAM	Mechanical attachment method
MWCNT	Multi-walled carbon nanotubes
NaCl	Sodium chloride
Na ₂ HPO ₄	Sodium dihydrogen orthophosphate
NaOH	Sodium hydroxide
NH ₄ Cl	Ammonium chloride
HNO ₃	Nitrogen acid
Ox	Oxidation
Pt	Platinum
PBS	Phosphate buffer solution
RE	Reference electrode
Red	Reduction
SEM	Scanning electron microscopy
SCM	Solvent casting method
SPV	Solid phase voltammetry
SWCNT	Single-walled carbon nanotubes
TiO ₂	Titanium dioxide
UV	Ultraviolet
WE	Working electrode

1.2 Nanostructured Material Modified Electrode

In recent years, the attention has been focused on growth of modified electrodes based on various nanostructured materials such as nanotubes, nanofibers, nanowires, nanoballs and nanoparticles. Nanostructured material modified electrodes can offer great benefits in electroanalytical research and application because of their great advantages of high effective surface area, mass transportation, catalysis and control over microenvironment (Katz *et al.*, 2004).

Increasing the electroactive surface area can be achieved by the attachment of nanostructures materials onto electrode surface. The large effective surface area may also cause there to be a larger number of active sites and often a higher signal to noise ratio (Welch and Compton, 2006). This increased electroactive surface area allows lower detection limit and higher sensitivity to analytes. The main challenge in achieving a high surface area electrode is the control over the size and distribution of the structures produced on the electrode. Thus enhanced mass transport of nanostructured electrodes, due to dominance of radial diffusion, decreased charging currents and deleterious effects of solution resistance. They may be defined as electrodes with a critical dimension in the nanometer range (1 nm –100 nm), where by critical dimension is meant that dimension which controls the electrochemical response (Arrigan, 2004). Conversely, the catalytic properties of some nanoparticles can cause a decrease in the over potential needed for a reaction to become kinetically viable, producing voltammetry which appears more reversible.

1.3 Carbon Nanotubes

CNT are long cylindrical structure of 3-coordinated carbon, slightly pyramidalized by curvature from the pure sp^2 hybridization of graphene, toward the diamond-like sp^3 (Fischer, 2006). CNT present a seamless structure with hexagonal 'helicity' of the carbon honeycomb lattices (Lambin *et al.*, 2002), being several nanometers in diameter and many microns in length (Ajayan, 1999). CNT are closed structures that present two well defined regions with clearly different properties, the tube and the cap, which is hemi-fullerenes-like molecule with topological defects that in this case are mainly pentagons (Rivas *et al.*, 2007).

There are two basic types of CNT, namely single-walled carbon nanotubes (SWCNT) and multi-walled carbon nanotubes (MWCNT) as shown in Figure 1.1. SWCNT consist of a single graphite sheet rolled seamlessly defining a cylinder of 1-2 nm diameter. The minimum diameter of stable free standing SWCNT is limited by curvature-induced strain to 0.4 nm. Meanwhile, MWCNT can be visualized as concentric and closed graphite tubules with multiple layers of graphite sheets that define a hole of 2 - 25 nm separated by a distance of 0.34 nm (Fischer, 2006).

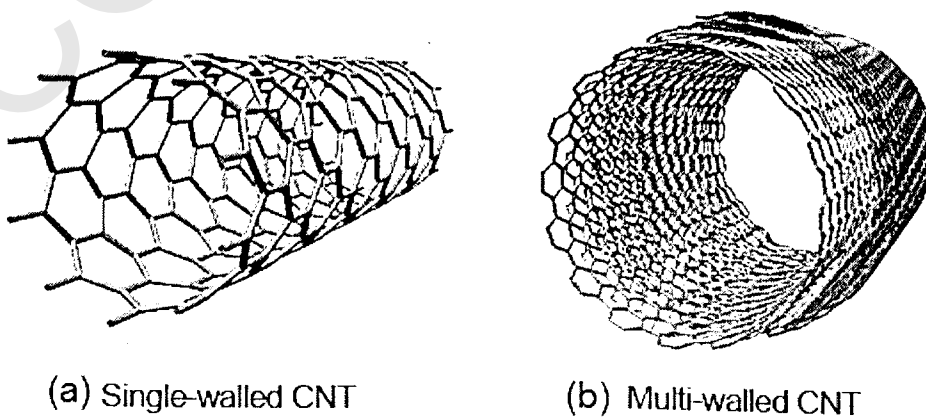


Figure 1.1. Scheme of single-walled (a) and multi-walled (b) carbon nanotubes

1.4 Titanium Dioxide

Titanium (iv) dioxide or titania, is well known as a white pigment, is the naturally occurring oxide of titanium with a chemical formula of TiO_2 . Titania has a number of crystalline forms such as rutile, anatase and brookite. Those all crystalline structures contain six-coordinate titanium and shown in Figure 1.2.

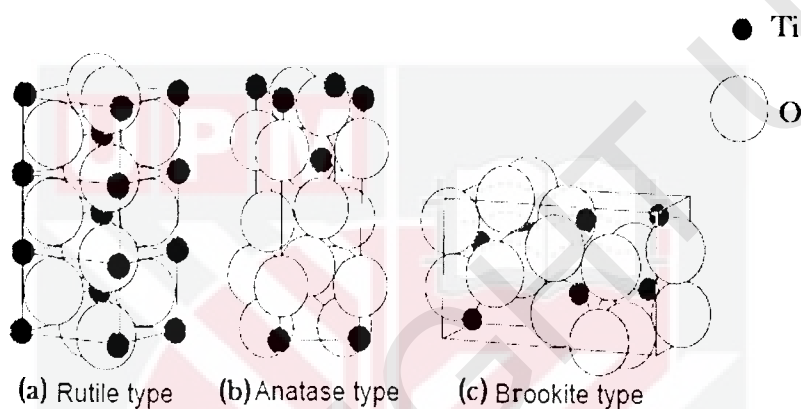


Figure 1.2. TiO_2 crystal structures: tetragonal (a), tetragonal (b) and orthorhombic (c)

Both anatase and brookite can be converted to rutile upon heating. The structure of anatase can be regarded to be built from octahedral connecting by vertices. In rutile, the edges are connected where as in brookite, both vertices and edges are connected. Anatase forms are shown to be more stable, photochemistry, active, and sensitive for catalyzed photodegradation. Meanwhile, rutile forms exhibit photochemical nature and relatively inactive. Brookite has less commercial importance.

1.5 Ascorbic Acid

L-ascorbic acid or L-3-ketothreohexuronic acid lactone, well known as vitamin C is usually prepared by synthesis from glucose, or extracted from plant sources like rose hips, blackcurrants or citrus fruits. It is used for the prevention and treatment of cold, fever, mental illness, infertility, the healing of wounds, elasticity of the skin, aids the absorption of iron and improves resistance to infection. Chemical formula of ascorbic acid is $C_6H_8O_6$ and molecular structure is shown in Figure 1.3.

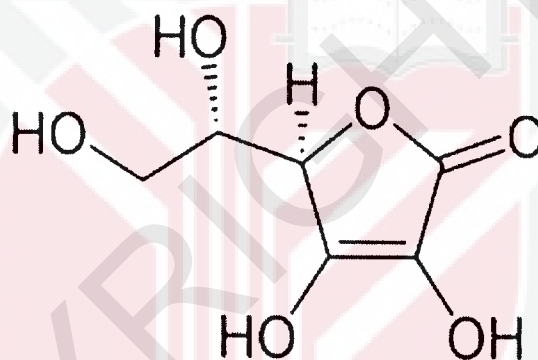


Figure 1.3. Molecular structure of ascorbic acid

Ascorbic acid is water soluble organic acid, that means human body does not store it automatically. Therefore, the supply must be taken daily either from food containing high vitamin C or supplements. There are many available sources in nature, from various kinds of food stuffs, which are rich in natural ascorbic acid, mostly rich in fresh fruits and leafy vegetables such as guava, papaya, cabbage and spinach (Goh *et al.*, 2008). Small amount can be also found from animal sources such as meat, fish, eggs and poultry. Among the all vitamins, ascorbic acid is the least stable vitamin, like easily oxidized in air and can be easily destroyed by heat and storage.

1.6 Paracetamol

Paracetamol (acetaminophen, 4-acetamidophenol, *N*-acetyl-*p*-aminophenol) is an antipyretic and analgesic drug, which was firstly introduced in medicine by Von Mering in 1893. It is commonly used to relieve pains such as aches, headaches, menstrual cramps and fever. Paracetamol is also used in combination with narcotic analgesics, which increases its efficacy and reduces the risk of narcotics abuse. It is sold under various brand names like Tylenol, Panadol and Aspirin-Free Anacin, usually formulated in tablets, containing 500 mg paracetamol per tablet. Molecular structure of paracetamol is similar to aspirin as shown in Figure 1.4.

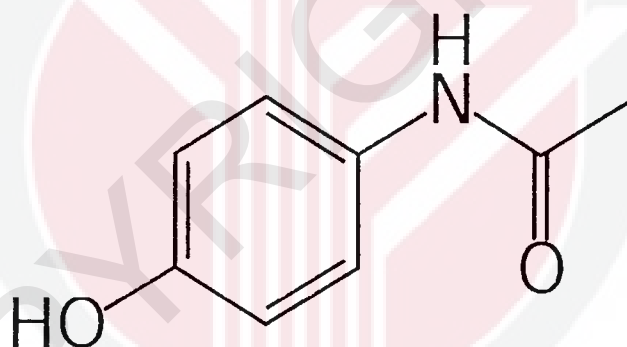


Figure 1.4. Molecular structure of paracetamol

Paracetamol is considered safe for human use when the recommended dose is not exceeded. But because of its wide availability, purposeful or accidental overdose is quite common. It is also used in suicide attempts, and in this respect it is potentially more dangerous than other over-the-counter drugs such as aspirin. This is because overdoses of paracetamol may cause nausea, vomiting, sweating, and exhaustion. Very large overdose can cause liver failure and death. Taken long-term, in proper therapeutic doses, the liver and also other organs can be harmed.

1.7 Fundamental of Voltammetric Techniques

Voltammetry is the branch of electrochemistry, which is one of the main analytical techniques. All areas of voltammetry (theory, methodology, and instrumentation) have been significantly advanced since when it developed from the discovery of polarography. Generally, voltammetry is based on the measure of the faradaic current passing through the electrolyte solution containing electro-active compounds while the time-dependent potential is applied to an electrode in electrochemical cell. A plot of current as a function of applied potential is called a voltammogram (Christian, 1994), which provides quantitative and qualitative information about the species involved in the reaction.

Solid phase voltammetry (SPV) or voltammetry of microparticles technique is used for solid state samples mechanically transfer onto the surface of the bare electrode and then forcing redox reaction to proceed. This method is designed to directly perform electrochemical studies of solid phases, such as metals and alloys, sparingly soluble complexes, organic compounds (Scholz and Lange, 1992). The simplicity and usefulness of the abrasion technique in SPV have been described (Scholz and Lange, 1992). Its usefulness includes the qualitative and quantitative identification of the constituents of alloys, minerals, pigments, corrosion processes and non-conducting organic and inorganic compounds. This technique is especially useful for the voltammetric studies of compounds that are insoluble.

1.7.1 Linear Sweep Voltammetry

Linear sweep voltammetry is the simplest voltammetric technique, which uses a linear potential ramp waveform. The current response is measured when the potential is applied to the working electrode as a function of time as shown in Figure 1.5.

The slope of this ramp has units of volts per unit time, and is generally called the scan rate of the experiment. With a linear potential ramp, the faradaic current is found to increase at higher scan rates. This is due to the increased flux of electroactive material to the electrode at the higher scan rates. The value of $E_{1/2}$ can be used to identify unknown species, and the height of the limiting current can be used to determine concentration.

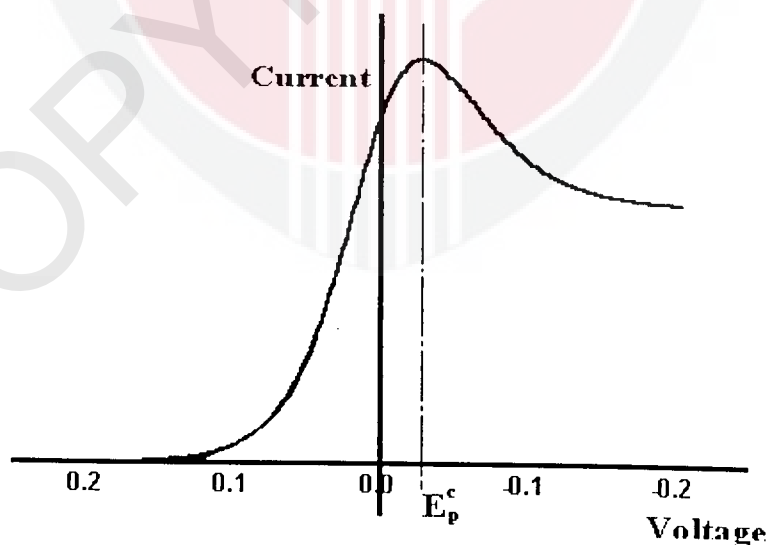


Figure 1.5. Linear sweep voltammetry

1.7.2 Cyclic Voltammetry

Cyclic voltammetry is widely used voltammetric technique, which is based on a linear potential waveform; the potential is changed as a linear function of time. It is useful for rapidly providing considerable information on the thermodynamics of redox processes, the kinetics of heterogeneous electron-transfer reactions, and on coupled chemical reactions or adsorption processes (Wang, 2000). The electrode potential is scanned linearly with a triangle wave form as shown in Figure 1.6.

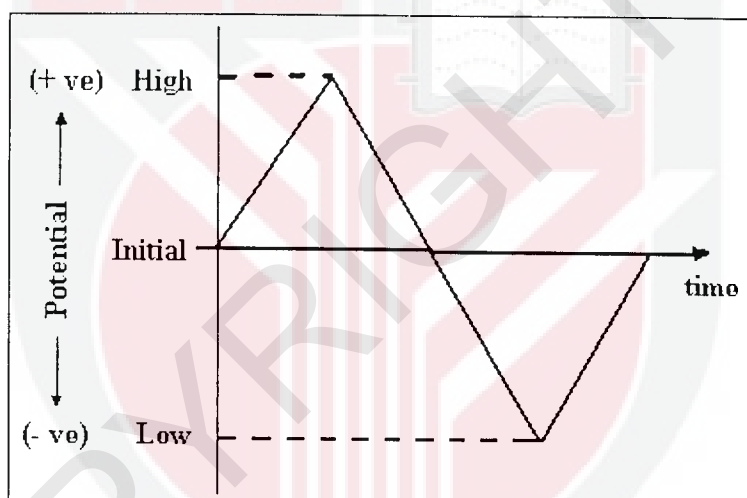


Figure 1.6. Triangular potential waveform for cyclic voltammetry

The important parameters of cyclic voltammogram are the peak currents and peak potentials of the anodic and cathodic peaks, respectively. If the heterogeneous electron transfer is rapid compared to the mass transfer, diffusion or migration flux of the reactants and products of the electrode reaction, the redox reaction is said to be electrochemically reversible (Girault, 2004). The peak current, in terms of the analyte concentration, for a reversible redox reaction at 25°C is given by Randles-Sevcik equation:

$$i_p = (2.69 \times 10^5) n^{3/2} ACD^{1/2} v^{1/2} \quad [1.1]$$

In this equation, n is the number of electron transferred per molecule (equiv/mole), v is the scan rate (V/s), A is the electrode surface area (cm²), D is the analyte's diffusion coefficient (cm²/s) and C is the analyte's concentration (mole/cm³).

Therefore, for a reversible reaction, the peak current is directly proportional to the concentration, and the square root of the scan rate. Meanwhile, the peak separation for a reversible redox reaction is given by:

$$\Delta E_p = E_{pa} - E_{pc} = 2.303 RT / nF \quad [1.2]$$

Thus, ΔE_p for a reversible redox reaction at 25°C should be 0.0592/nV. For irreversible or quasi-reversible redox reaction, ΔE_p should be greater than 0.0592/nV (Eklund *et al.*, 1999). The peak separation is useful in determining the number of electrons transferred, and as a criterion for Nernstian behavior (Wang, 2000). The formal reduction potential for a reversible redox couple is easily determined as the average of the two peak potentials as shown in Equation 1.3. Formal reduction potentials measured using cyclic voltammetry is usually accurate to within 50 mV of the true value.

$$E^\circ = (E_{pa} + E_{pc})/2 \quad [1.3]$$

In addition, in a reversible redox couple: $I_{pa}/I_{pc}=1$ for all scan rates. But, in the irreversible reaction, the potential peaks are reduced in size and widely separated. The extent of irreversibility increases with rises in sweep rate. The behaviors of irreversible process are caused by slow electron transfer kinetics and the chemical reaction of oxidation (Ox) and reduction (Red). For the quasi-reversible redox system, the current is controlled by both the charge transfer and mass transport.

1.7.3 Chronoamperometry

Chronoamperometry (CA) is a technique where the current is measured as a function of time under potentiostatic control. In CA, the excitation signal is a square-wave signal. The potential is stepped from an initial potential value at which there is no electrolysis to a final potential value (Figures 1.7) at which a diffusion-controlled oxidation or reduction occurs. The potential can be stepped back to initial potential after pulse width time and this technique is known as double-potential step CA.

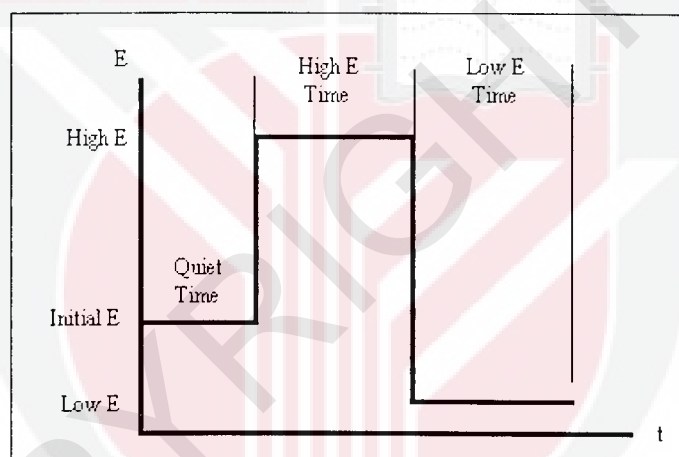


Figure 1.7. Potential waveform for chronoamperometry

In conjunction with Faraday's Law, the charge, Q , passed across the interface is related to the amount of material that has been converted, and the current is related to the instantaneous rate at which the conversion occurs. The current decays smoothly as the electrolysis proceeds to deplete the solution near the electrode of electroactive species. Since electron transfer occurs in a faradaic electrode process, the current is the faradaic current. The current response decays as a function of time for a planar electrode is expressed by the Cottrell equation (Brett & Oliveira-Brett, 1993):

$$i_f(t) = nFAC(D/\pi t)^{1/2} \quad [1.4]$$

Where, i_f is the Faradaic current (A), n is the number of electrons transfer per molecule (Equiv/mole), F is the Faraday's constant (96500 C/Equiv), A is the electrode area (cm²), C is the analyte's concentration (mole/cm³), D is the analyte's diffusion coefficient (cm²/s) and t is the time (s).

CA can be applied to determine diffusion coefficient, electrode area and electron stoichiometry and the study of mechanism of electrode process. These parameters were determined from the gradient of i versus $t^{-1/2}$ graph. CA is also used to determine the effective electrochemical area of an electrode, when D and n are known. Once the electrode area is known, the electrode can be used to measure the value for diffusion coefficient (Brett & Oliveira-Brett, 1993).

1.7.4 Chronocoulometry

Chronocoulometry (CC) is frequently used one of the classical voltammetric techniques; hence, the charge is monitored as a function of time. Figures 1.8 shows the chronocoulogram. In CC, the electrode is being applied a linear potential ramp or potential step at an initial potential, where no current flows to a final potential, where the reaction of interest does occur. This results in a passage of charge across the electrode interface. General process of CC is similar to CA, but the difference is the measurement of charge instead of current directly as in CA.

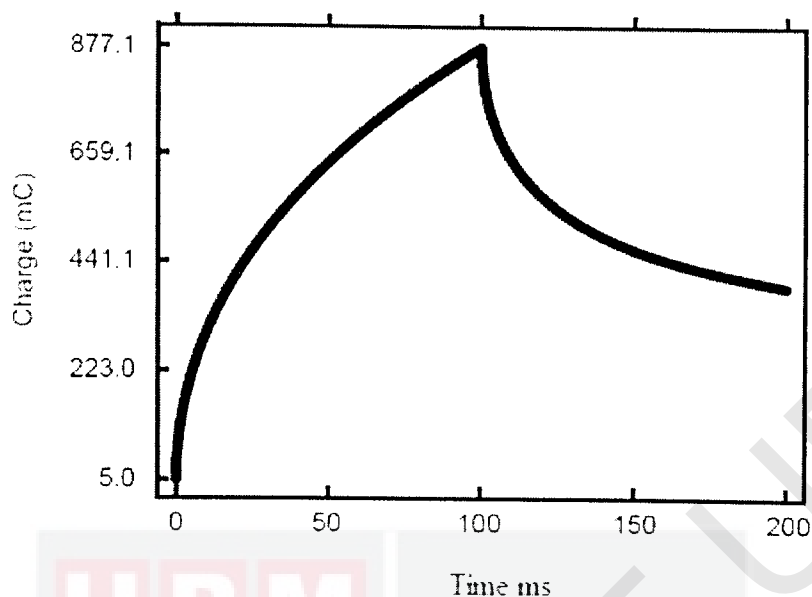


Figure 1.8. Chronocoulogram (charge-time) response for double potential step chronocoulometry

The expression for the forward chronocoulometric response of diffusing components is simply the Cottrell equation integrated with respect to time as shown below:

$$Q_d = 2nFAD^{1/2}C\pi^{-1/2}t^{1/2} \quad [1.5]$$

Where, Q_d is the diffusing charge (C), n is the number of electrons per molecule (Equiv/mole), F is the Faraday's constant (96500 C/Equiv), A is the electrode area (cm^2), C is the concentration of electroactive species (mole/cm^3), D is the diffusion coefficient of electroactive species (cm^2/s), t is the time (s).

One of the applications of CC is its ability to detect species absorbed onto the surface of the working electrode. Such species are electrolyzed very rapidly once the potential is stepped. In a simplified mathematical treatment, three sinks of charges are considered separately as additive function. The three charges are charge from the diffusing species due to the charging of working electrode, capacitive charge of the

electrode double layer, and adsorptive charge due to electrolysis of the adsorbed species. Among the three components, only Q_d is time independent. The total forward chronocoulometric response can thus be described by:

$$Q_{total} = Q_d + Q_{dl} + Q_{ads} \quad [1.6]$$

$$Q_{total} = 2nFAD^{1/2}C\pi^{-1/2}t^{1/2} + Q_{dl} + nFA\Gamma \quad [1.7]$$

Where, Q_{total} is the total charge and Γ is the surface excess of reactant (mole/cm²).

According to the equation above, the plot of Q versus $t^{1/2}$ should be linear and the linearization of the chronocoulometric response by CC is illustrated in Figure 1.14. This plot is often referred as Anson plot. The slope of this line is $2nFAD^{1/2}C\pi^{-1/2}\pi$ and the intercept is $Q_{dl} + nFA\Gamma$ (Wang, 2000). It is useful to step the potential back to the initial potential, and then record the charge due to the reaction of the species produced on the forward step. The expression of the reverse step is shown in Equation 1.8.

$$Q_r = 2nFAD^{1/2}C\pi^{-1/2}\theta + Q_{dl} + nFA\Gamma_r \quad [1.8]$$

Where, Q_r is equal to $Q_{max} - Q_t$, θ is equal to $(\tau^{1/2} + t - \tau^{1/2} - t^{1/2})$, τ means the forward step width and t is the total integration time.

The capacitive charge is eliminated to yield $nFA(\Gamma_o - \Gamma_r)$ when the intercept of the forward step subtracts the intercept of the reverse step. If only one species adsorbs, this then gives that species' surface excess directly.

1.8 Problem Statement

In recent years, electroanalysts are focused on development of new chemically modified electrodes, because currently available working electrodes such as glassy carbon, gold and platinum are lack of sensitivity and selectivity (Gooding, 2005). The new electrode should be able to possess following advantages: highly sensitive, good detection limit, stability, selectivity, reproducibility, low cost and simplicity. Recent published works used GCE modified with a thin layer or film of CNT (Dai, 2006). Typically using CNT modified GCEs for electroanalysis the claimed benefits include good detection limits, increased sensitivity, resistance to surface fouling and decreased overpotentials (Wang, 1995).

Combining the unique properties of CNT, such as high specific surface area, subtle electronic properties and strong adsorptive ability, with nanostructured TiO_2 as a composite material is expected to enhance the electrocatalytic activity of CNT/GCE. To date, there are no published reports on the usage of CNT/ TiO_2 nanoparticle composite modified GCE. Therefore the main objectives of the present study were to develop new chemically modified electrode based on the CNT/ TiO_2 /GCE. The outcomes of this research will have substantial contribution to the field of electrochemical and nanosciences.

1.9 Objectives

The objectives of this study are:

- i. To fabricate a chemically modified electrode based on the CNT/TiO₂/GCE composite using solution evaporation and mechanical attachment methods.
- ii. To characterize the composite electrode using scanning electron microscopy, energy dispersive X-ray, and voltammetric techniques of cyclic voltammetry, linear sweep voltammetry, chronoamperometry and chronocoulometry.
- iii. To compare the electrode responses of the CNT/TiO₂/GCE composite with that CNT/GCE; TiO₂/GCE and unmodified GCE in order to determine some biological and chemical analytes.
- iv. To determine the optimum physical and chemical conditions under which maximum current enhancement can be obtained for the electrochemical response of above analytes.

REFERENCES

- Agüí, L., Yáñez-Sedeño, P. and Pingarrón, J.M. (2008). Role of carbon nanotubes in electroanalytical chemistry: *Analytica Chimica Acta* 622 (1-2): 11-47.
- Ahmmad, B., Kusumoto, Y., Somekawa, S. and Ikeda, M. (2008). Carbon nanotubes synergistically enhance photocatalytic activity of TiO₂. *Catalysis Communications* 9 (6): 1410-1413.
- Ajayan, P.M. (1999). Nanotubes from carbon. *Chemical Reviews* 99 (7): 1787-1800.
- Alkire, R.C., Kolb, D.M. and Lipkowski, J. (2009). Chemically modified electrodes. Wiley-VCH.
- An, L.P., Gao, X.P., Li, G.R., Yan, T.Y., Zhu, H.Y. and Shen, P.W. (2008). Electrochemical Lithium Storage of Titania Nanotubes modified with NiO Nanoparticles. *Electrochimica Acta* 53: 4573-4579.
- Arrigan, D.W.M. (2004). Nanoelectrodes, nanoelectrode arrays and their applications. *The Analyst*, 129 (12): 1157-1165.
- Banks, C.E., Davies, T.J., Wildgoose, G.G. and Compton, R.G. (2005). Electrocatalysis at graphite and carbon nanotube modified electrodes: edge-plane sites and tube ends are the reactive sites. *Chemical Communications* 7: 829-841.
- Bard, A.J. and Faulkner, L.R. (2001). *Electrochemical Methods, Fundamentals and Application*. Wiley, New York.
- Barteau, M.A. (1993). Site requirements of reactions on oxide surfaces. In *39th National Symposium of the American Vacuum Society* 11: 2162-2168.
- Baughman, R.H., Zakhidov, A.A. and de Heer, W.A. (2002). Carbon Nanotubes--the Route Toward Applications. *Science* 297 (5582): 787-792.
- Bethune, D.S., Klang, C.H., de Vries, M.S., Gorman, G., Savoy, R., Vazquez, J. and Beyers, R. (1993). Cobalt-catalysed growth of carbon nanotubes with single-atomic-layer walls. *Nature* 363 (6430): 605-607.
- Brett, C.M.M. and Oliveira-Brett, A.M. (1993). *Electrochemistry Principles, Methods, and Applications*. Oxford University Press Inc., Oxford.
- Bruce, P.G. (1995). *Solid State Electrochemistry*. Cambridge University Press, Cambridge.
- Chen, Y., Crittenden, J.C., Hackney, S., Sutter, L. and Hand, D.W. (2005). Preparation of a Novel TiO₂-Based p-n Junction Nanotube Photocatalyst. *Environmental Science & Technology* 39 (5): 1201-1208.

- Christian, C.D. (1994). *Analytical Chemistry*, fifth edition. New York: John Wiley and Sons. Inc
- Curulli, A., Valentini, F., Padeletti, G., Viticoli, M., Caschera, D. and Palleschi, G. (2005). Smart (Nano) materials: TiO₂ nanostructured films to modify electrodes for assembling of new electrochemical probes. *Sensors and Actuators B* 111-112: 441-449.
- Dai, X., Wildgoose, G.G. and Compton, R.G. (2006). Apparent 'electrocatalytic' activity of multiwalled carbon nanotubes in the detection of the anaesthetic halothane: occluded copper nanoparticles. *Analyst* 131: 901-6.
- Davis, J.J., Coleman, K.S., Azamian, B.R., Bagshaw, C.B. and Green, M.L.H. (2003). Chemical and Biochemical Sensing with Modified Single Walled Carbon Nanotubes. *Chemistry - A European Journal* 9 (16): 3732-3739.
- Diebold, U. (2003). The surface science of titanium dioxide. *Surface Science Report* 48 (5-8): 53-229.
- Ebbesen, T.W. and Ajayan, P.M. (1992). Large-scale synthesis of carbon nanotubes. *Nature* 358 (6383): 220-222.
- Eklund, J.C., Bond, A.M., Alden, J.A. and Compton, R.G. (1999). Perspectives in Modern Voltammetry: Basic Concepts and Mechanistic Analysis. *Advances in Physical Organic Chemistry* 32: 1-120.
- Fischer, J.E. (2006). Carbon Nanotubes: Structure and Properties. In Yuri Gogotsi (Ed.), *Nanotubes and Nanofibers* (Chap. 1). CRC Press, Boca Raton.
- Fujishima, A., Zhang, X. (2006). Titanium dioxide photocatalysis: present situation and future approaches. *Comptes Rendus Chimie* 9 (5-6): 750-760.
- Fujishima, A., Hashimoto, K., and Watanabe, T. (2000). Mechanism of Photocatalyst. Nippon Jitsugyo Publishing Co., Tokyo.
- Gao, B., Chen, G.Z. and Li, P.G. (2009). Carbon nanotubes/titanium dioxide (CNTs/TiO₂) nanocomposites prepared by conventional and novel surfactant wrapping sol-gel methods exhibiting enhanced photocatalytic activity. *Applied Catalysis B: Environmental* 89 (3-4): 503-509.
- Girault, H.H. (2004). *Analytical and Physical Electrochemistry*. EPFL Press, Switzerland.
- Gooding, J.J. (2005). Nanostructuring electrodes with carbon nanotubes: A review on electrochemistry and applications for sensing. *Electrochimica Acta* 50: 3049-3060
- He, D., Yang, L., Kuang, S. and Cai, Q. (2007). Fabrication and catalytic properties of Pt and Ru decorated TiO₂/CNTs catalyst for methanol electrooxidation. *Electrochemistry Communications* 9: 2467-2472.

- Iijima, S. (1991). Helical microtubules of graphitic carbon. *Nature* 354 (6348): 56-58.
- Iijima, S. and Ichihashi, T. (1993). Single-shell carbon nanotubes of 1-nm diameter. *Nature* 363 (6430): 603-605.
- Jiang, L. and Zhang, W. (2009). Electrodeposition of TiO₂ nanoparticles on multiwalled carbon nanotube arrays for hydrogen peroxide sensing. *Electroanalysis* 21 (8): 988-993.
- Journet, C., Maser, W.K., Bernier, P., Loiseau, A., Chapelle, L., Lefrant, S.M., Deniard, P., Lee, R. and Fischer, J.E. (1997). Large-scale production of single-walled carbon nanotubes by the electric-arc technique. *Nature* 388: 756-758.
- Katz, E., Willner, I. and Wang, J. (2004). Electroanalytical and bioelectroanalytical systems based on metal and semiconductor nanoparticles. *Electroanalysis*, 16 (1-2): 19-44.
- Koelsch, M., Cassaignon, S., Ta Thanh Minh, C., Guillemoles, J. and Jolivet, J. (2004). Electrochemical comparative study of titania (anatase, brookite and rutile) nanoparticles synthesized in aqueous medium. *Thin Solid Films* 451-452 (22): 86-92.
- Lambin, P., Loiseau, A., Culot, C. and Biró, L.P. (2002). Structure of carbon nanotubes probed by local and global probes. *Carbon* 40 (10): 1635-1648.
- Li, M., Hu, Z., Wang, X., Wu, Q., Chen, Y. and Tian, Y. (2004). Low-temperature synthesis of carbon nanotubes using corona discharge plasma at atmospheric pressure. *Diamond and Related Materials* 13 (1): 111-115.
- Li, Y., Kinloch, I.A., Shaffer, M.S.P., Geng, J., Johnson, B. and Windle, A.H. (2004). Synthesis of single-walled carbon nanotubes by a fluidized-bed method. *Chemical Physics Letters* 384 (1-3): 98-102.
- Musameh, M., Lawrence, N.S. and Wang, J. (2005). Electrochemical activation of carbon nanotubes. *Electrochemistry Communications* 7 (1): 14-18.
- McCall, M.R. and Frei, B. (1999). Can antioxidant vitamins materially reduce oxidative damage in humans? *Free Radical Biology & Medicine* 26 (7-8): 1034-1053.
- Pang, X., He, D., Luo, S. and Cai, Q. (2009). An amperometric glucose biosensor fabricated with Pt nanoparticle-decorated carbon nanotubes/TiO₂ nanotube arrays composite. *Sensors and Actuators B: Chemical* 137 (1): 134-138.
- Rivas, G.A., Rubianes, M.D., Rodriguez, M.C., Ferreyra, N.F., Luque, G.L., Pedano, M.L., Miscoria, S.A. and Parrado, C. (2007). Review: Carbon nanotubes for electrochemical biosensing. *Talanta* 74: 291-307.

- Sawatsuk, T., Chindaduang, A., Sae-kung, C., Pratontep, S. and Tumcharern, G. (2009). Dye-sensitized solar cells based on TiO₂-MWCNTs composite electrodes: Performance improvement and their mechanisms. *Diamond and Related Materials* 18 (2-3): 524-527.
- Scholz, F. and Lange, B. (1992). Abrasive stripping voltammetry – An electrochemical solid state spectroscopy of wide applicability. *Trends in Analytical Chemistry* 11 (10): 359-367.
- Song, H., Qiu, X. and Li, F. (2008). Effect of heat treatment on the performance of TiO₂-Pt/CNT catalysts for methanol electro-oxidation. *Electrochimica Acta* 53: 3708-3713.
- Goh, J.K., Tan, W.T., Lim, F.T. and Maamor, N.A.M. (2008). Electrochemical oxidation of ascorbic acid mediated by a carbon nanotubes/Li⁺ modified graphite electrode. *The Malaysian Journal of Analytical Sciences* 12 (2): 480 - 485.
- Thess, A., Lee, R., Nikolaev, P., Dai, H., Petit, P., Robert, J., Xu, C., Lee, Y.H., Kim, S.G., Rinzler, A.G., Colbert, D.T., Scuseria, G.E., Tomane'k, D., Fischer, J.E. and Smalley, R.E. (1996). Crystalline ropes of metallic carbon nanotubes. *Science* 273: 483-487.
- Vivekchand, S.R.C., Cele, L.M., Deepak, F.L, Raju, A.R. and Govindaraj, A. (2004). Carbon nanotubes by nebulized spray pyrolysis. *Chemical Physics Letters* 386 (4-6): 313-318.
- Wang, J. (2000). *Analytical Electrochemistry*. VCH Publishers, New York.
- Wang, J. Li, M., Shi, Z., Li, N. and Gu, Z. (2002). Direct electrochemistry of cytochrome *c* at a glassy carbon electrode modified with single-wall carbon nanotubes. *Analytical Chemistry* 74 (9): 1993-1997.
- Welch, C. and Compton, R. (2006). The use of nanoparticles in electroanalysis: a review. *Analytical and Bioanalytical Chemistry* 384 (3): 601-619.
- Wildgoose, G.G., Banks, C.E., Leventis, H.C. and Compton, R.G. (2006). Chemically modified carbon nanotubes for use in electroanalysis. *Microchimica Acta* 152 (3): 187-214.
- Xia, X., Jia, Z., Yu, Y., Liang, Y., Wang, Z. and Ma, L. (2007). Preparation of multi-walled carbon nanotube supported TiO₂ and its photocatalytic activity in the reduction of CO₂ with H₂O. *Carbon* 45 (4): 717-721.
- Yacaman, M.J., Yoshida, M.M., Rendon, L., Santiesteban, J.G. (1993). Catalytic growth of carbon microtubules with fullerene structure. *Applied Physics Letters* 62 (2): 202-204.
- Yu, H., Quan, X., Chen, S., Zhao, H. and Zhang, Y. (2008). TiO₂-carbon nanotube heterojunction arrays with a controllable thickness of TiO₂ layer and their

first application in photocatalysis. *Journal of Photochemistry and Photobiology A: Chemistry* 200 (2-3): 301-306.

Zhang, M., Gong, K., Zhang, H. and Mao, L. (2005). Layer-by-layer assembled carbon nanotubes for selective determination of dopamine in the presence of ascorbic acid. *Biosensors and Bioelectronics* 20 (7): 1270-1276.

